J Math Chem (2012) 50:949–970
DOI 10.1007/s10910-011-9942-0

ORIGINAL PAPER

Constructing quantum mechanical models starting from diabatic schemes: Quantum states for simulations bond break/formation—I. Feshbach-like quantum states and electronuclear wave functions

Gustavo A. Arteca · Josep M. Aulló · O. Tapia

Received: 11 October 2011 / Accepted: 22 October 2011 / Published online: 12 November 2011

Abstract A quantum description adapted to scrutinize chemical reaction mechanisms obtains by implementing an electronuclear separation via quantum numbers method; truly diabatic base states obtain that sustain quantum states expressed as linear superpositions. A proto-type bond breaking/formation case: $H_2^+ \Leftrightarrow H(1s) + H^+$ test possibilities via mathematical modeling. Asymptotic states ($|H\rangle \otimes |H^+\rangle$) and ($|H^+\rangle \otimes |H\rangle$) and basis states for quantized electromagnetic radiation complete the model; Feshbach-resonance-like quantum states obtain that play pivotal roles gating association/dissociation processes. A fixed grid of floating Gaussian orbitals permits actual computations compatible with this method. The information therefrom gleaned is used to construct model Hamiltonians easily adaptable to second quantization formalisms. Theoretical developments and non-routine computations results can directly be related to experiment.

Keywords Feshbach states · Quantum states for chemical processes · Entanglements and reaction mechanisms · Floating Gaussian grid algorithm

G. A. Arteca
Département de Chimie et Biochimie & Biomolecular Sciences Programme, Laurentian University, Ramsey Lake Road, Sudbury, ON, P3E 2C6, Canada

G. A. Arteca · O. Tapia (✉)
Department of Physical and Analytical Chemistry, Uppsala University, Box 259, 751 05 Uppsala, Sweden
e-mail: orlando.tapia@fki.uu.se

J. M. Aulló · O. Tapia
Departament de Química Física, Universitat de València, Dr. Moliner 50, 46100 Burjassot, Valencia, Spain

1 Introduction

The development of diabatic schemes serving as a ground to formulate a quantum theory of chemical reactions has been one of our continued focus of interest [1–9]. Besides, quantum technology at laboratory level is producing important progress [10–17] and, as a result, the way we quantum chemists look at simple chemical systems has begun to be turned upside down. Use of molecular states to encode quantum information [10,11], as well as confining techniques (e.g., optical [12] or chip-based micro-traps [13,14]) open possibilities for changing molecular responses (properties); external electric and magnetic fields allow for modulation and manipulation of molecular quantum states including the tuning of reaction mechanisms [15]. A by-product of this would be the ability to overcome pathways via forbidden transitions [16], thereby opening possibilities to find paths to new chemical species that otherwise cannot be achieved by conventional thermal or photochemical means [17]. On the theoretical side, mechanistic descriptions of poly-electronic system would most likely require mixing of base states with different total angular momenta as discussed e.g. in ref. [18] thereby overcoming some severe limitations in the present computing state of affairs.

Thus, understanding the phenomena above requires a fair amount of quantum mechanical concepts that are not available from standard computational-chemistry technology based on Born-Oppenheimer (BO) adiabatic model. Such an approach leads to classical potential energy surfaces (PES); in particular, implementations with atomic (Gaussian) orbitals attached at nuclei may conceal hidden difficulties when handling mechanistic studies of bond break/forming as shown by Crespo et al. [19]; see also references therein where detailed discussions can be found [19]. Now, even in the simple H+H reaction, BO-PES generated with standard computational algorithms do not produce a mechanism consistent with the experimental observations. Thus, it is more and more apparent that proper quantum counterparts must somehow replace inadequate classical mechanical models; see ref. [8] for comparisons. The present paper, starting from diabatic perspectives, moves forward the mathematical formalism and prepares it to explore electronuclear separability via a new perspective: namely, quantum numbers [1,20,21]. The separability by quantum numbers provides, in principle, a chemically flavored basis set as illustrated below. Furthermore, this basis set concept prompts for extensions towards formalisms based on second quantization schemes that can be adapted fairly easily thereby opening new applicability domains.

The system $H_2^{\cdot} \rightleftarrows H(1s) + H^{\cdot}$ stands out as a model prototype adaptable to studies of generic chemical bond break/forming processes describable as bond altering ones; from the physical point of view, it involves notions at a fundamental quantum physical level including quantum entanglement. Here we extend and develop the quantum treatment given in ref. [1] for isomerization processes along two directions: (1) inclusion of asymptotic states needed to model a bimolecular and/or unimolecular decomposition reactions; (2) introduction of quantized electromagnetic (EM) fields [22]; the latter are fundamental information carriers [20,21]. The system is simple enough to allow illustrating the main aspects of quantum states underlying the phenomena. Here, the wheeling concept requires quantum physics of systems coupled to external probing

sources; this is in contrast the traditional PESs [23] (see also [2–9]) that play now a subsidiary (yet illustrative) role via diabatic procedures.

Section 2 situates the problem; it starts from the notion that molecular (coherent) quantum states, expressed as linear superpositions over basis states. Quantum states for chemical processes are introduced; information over such states can be gathered from conveniently adapted quantum-chemical models. It is worth noting that the concept of quantum state differs from the standard one; to avoid lost in focus in references [20,21] we discuss the issue at length. Qualitative discussion of quantum states variations simulating chemical processes permits illustrating the abstract theoretical approach including the role of Feshbach type resonance [24] that here are expressed as Feshbach quantum states.

Section 3 summarizes the practical method used to introduce molecular quantum states and briefly shows the construction of *ab initio* electronic basis functions needed to model bond altering processes.

A two-state model for dissociative reaction $H_2^+ \rightarrow H(1s) + H^+$ based on floating Gaussian approach numerically illustrate possible results; connection with experimental results is examined. We comment on the role of an external field to modulate bond altering and possibly leading to the formation of an effective reaction barrier.

Section 4 rounds up the theoretical scheme by introducing Hamiltonian representations that include features of the semi-classic scheme via quantum numbers. Model Hamiltonians are defined that help discussing situations related to laboratory experiments.

Conclusions are presented in Sect. 5.

2 Molecular electronuclear basis states

Diabatic schemes are well known within semi-classic frameworks [2,8] albeit here they are not end points but instead they help beginning the construction of molecular quantum mechanical schemes.

To get a fresh start in mathematical terms it is necessary to construct mappings relating abstract quantum states formalism [20,21] to particular theories covering quantum states sustained by matter with a well-defined number of basic constituents, namely, electrons and nuclei. It results in the construction of electrons-nuclei separation via a procedure based on quantum numbers [1] that departs from the mechanical one followed in the BO model [23]; the path followed and potentialities are illustrated with the help of refs. [2–9] and references therein. Here, for the sake of completeness, an overview with fresh ideas is presented. These latter are required because the target level corresponds to laboratory floor where quantum states sustained by material systems are probed (measured) by quantum physical systems and eventually recorded [20].

A "quantum probe", e.g., quantized electromagnetic radiation, can be thought as a generic device that drives a material system, yet not the particles but the quantum state. Thus, when a chemical process is subject to "probing," one induces responses originated in time-dependent quantum states [1,20,21]. Our goal is to characterize these quantum states, and monitor their behavior in terms of quantum-state *amplitudes*.

2.1 Abstract framework

Bridging abstract formalism in Hilbert space to one projected at a laboratory level is the principal target; this might help sensing where the problems are when coming to probing laboratory systems.

Consider a general material system, defined by its number of electrons (n) and nuclei (N), in addition to a time-independent Hamiltonian $\hat{H}$. Let $\{|j\rangle\}$ and $\{\varepsilon_j\}$ be the corresponding complete set of basis states with respective eigenvalues. Any quantum state for this system is a $|\Psi, t\rangle$-ket written as a linear superposition with complex number amplitudes $\{C_j\}$:

$$|\Psi, t\rangle = \sum_j C_j(\Psi, t)|j\rangle = (|1\rangle \ldots |j\rangle \ldots) \cdot \left(C_1 \ldots C_j \ldots\right)^t. \tag{1}$$

Consider an elementary transition from an "initial" (root) state $|k'\rangle$ towards a target state $|k\rangle$. If $|k\rangle\langle k'|$ is the excitation operator for this $k' \rightarrow k$ transition, the $[\hat{H}, |k\rangle\langle k'|]$-commutator provides information on the possible response of the $|\Psi, t\rangle$-ket projected over $|k\rangle$:

$$\langle k|[\hat{H}, |k\rangle\langle k'|]|\Psi, t\rangle = (\varepsilon_k - \varepsilon_{k'})C_{k'}(\Psi, t). \tag{2}$$

The amplitude at the initial state $|k'\rangle$(i.e., $C_{k'}(\Psi, t)$) will modulate the response and Bohr's postulate permits matching the Hilbert space gap $(\varepsilon_k - \varepsilon_{k'})$ with EM-radiation at frequency ω at a laboratory setup; information transmission and production is hence involved. Only nonzero amplitudes will yield a response at probing time with the appropriate frequencies.

Yet "probing" is not an operation in Hilbert space of $\{|k\rangle\}$-kets.

To achieve probing representation, an *external* source needs to be switched on [20,21]. Once this interaction source is included and allowed to interact, the resulting physical state will be given as linear superpositions similar to Eq. (1). The amplitudes register the changes.

We effectively try now opening a connection to laboratory systems. The representation in abstract Hilbert space is hence mapped to laboratory space by defining a "fence region" [20]. This "fence connection" is made within the framework of special relativity theory [21]. An inertial frame (I-frame) allows us to introduce space-time coordinates; time t appears as a parameter in Eq. (1), while space enters as Euclidean coordinates $\mathbf{x} = (\mathbf{x}_1, \ldots, \mathbf{x}_{n+1}, \ldots, \mathbf{x}_{n+N})$; *the number of degrees of freedom* determines the dimension of this abstract vector space. While I-frames' origin and relative orientations belong to laboratory space, $\mathbf{x}$-vectors belong to an abstract Cartesian product space used to label configuration kets $\{|\mathbf{x}\rangle\}$ that in turn define a "rigged Hilbert space" [22]. (For the sake of simplicity, spin degrees of freedom are not explicitly considered at this point.) Finally, a Hamiltonian introduces the parameters defining the material system; projecting abstract quantum states with $\{|\mathbf{x}\rangle\}$-set wave functions obtain:

$$\text{"Projection"} \text{ of } |\Psi\rangle \rightarrow \langle \mathbf{x}|\Psi\rangle \rightarrow \Psi(\mathbf{x}),$$

$\langle \mathbf{x}|\Psi\rangle$ is a complex (generalized) function over real number support; in mathematic notation: $\Psi(\mathbf{x})$.

Note, $d\mathbf{x}|\mathbf{x}\rangle\langle\mathbf{x}|\Psi\rangle$ stands out as a coded information of the quantum state in the hyper-volume $d\mathbf{x}$ around a configuration space point $\mathbf{x}$. The set $\{\Psi(\mathbf{x})\}$ still is an abstract Hilbert space. Note that there are an infinite number of quantum states and a finite number of material elements. The only requirement on the quantum state is that it is sustained by the materiality contained in the total given volume; there is no way to further localize the matter content, only its presence is required. This is a clear difference compared to standard theory.

A concept of *molecular structure* lacks in this context because $|\Psi, t\rangle$ and $\Psi(\mathbf{x})$ are functions supported by an abstract space $\{\mathbf{x}\}$. Only a semiclassic framework would permit structural definitions concerning elements of real space where an I-frame is planted [19].

Formally, the I-frame "localizes" a projected quantum $|\Psi, t\rangle$-state through complex functions $\langle\mathbf{x}|\Psi, t\rangle$; the abstract $\{|j\rangle\}$-kets are mapped onto the set of basis functions $\{f_j(\mathbf{x}) = \langle\mathbf{x}|j\rangle\}$; the amplitudes in Eq. (1) remain the same after this operation. The scalar product $(f_1(\mathbf{x})\ldots f_j(\mathbf{x})\ldots)\cdot(C_1\ldots C_j\ldots)^t$ represents the quantum state in the projected basis set.

A first level of chemical information is introduced by partitioning the $\mathbf{x}$-configurations formally into electron and nuclear degrees of freedom: $\mathbf{q} = (\mathbf{q}_1, \ldots \mathbf{q}_n)$ and $\boldsymbol{\xi} = (\boldsymbol{\xi}_1, \ldots, \boldsymbol{\xi}_N)$, respectively. The generic basis functions are not separable, yet quantum numbers are made distinct based on experimental experience. Therefore, the labels of basis functions can then be cast as: $f_j(\mathbf{x}) \rightarrow f_{k,g(k)}(\mathbf{q},\boldsymbol{\xi})$, where the quantum numbers distinguish between electronic (k) and subsidiary nuclear elements $(g(k))$. In principle, this spectroscopic labeling does not detract from the basis set completeness.

2.2 Molecular bases: semiclassical framework

Following basic ideas from refs. [1–9,20] exact basis states $f_{k,g(k)}(\mathbf{q}, \boldsymbol{\xi})$ can be the place for further modeling. For example, we consider here mappings introducing electronuclear separation by quantum numbers [1]:

$$f_{k,g(k)}(\mathbf{q}, \boldsymbol{\xi}) \rightarrow \psi_k(\mathbf{q})\, X_{g(k)}(\boldsymbol{\xi}). \tag{3}$$

A second level of chemical information employs the nuclear $\boldsymbol{\xi}$-configuration space. This can be taken as, either a geometric nuclear position space when standard quantum chemical algorithms are used; or once quantum numbers are selected its abstract nature must be restored to get electro-nuclear wave functions. The choice depends upon the problem under study; in contrast, $\mathbf{q}$-space retains its abstract meaning and only quantum numbers are meaningful.

The quantum state now takes on the form:

$$\langle \mathbf{q}, \boldsymbol{\xi}|\Psi, t\rangle \approx \sum_k \sum_{g(k)} C_{k,g(k)}(\Psi, t)\psi_k(\mathbf{q})\, X_{g(k)}(\boldsymbol{\xi}). \tag{4}$$

The quantum number $g(k)$ identifies basis functions that, though related to nuclear degrees of freedom, are strictly not separable from the electronic part; i.e. nuclei never "move as particles" [20,21]. The order chosen for $(\mathbf{q},\boldsymbol{\xi})$-space is fixed. In the semiclassic model the resulting $\boldsymbol{\xi}$-configuration space may include information on "stationary nuclear geometries" [2,7–9]. An important restriction remains however intact: no attempt is made at describing "particle electronic motion" [20,21]. The concern is about changes of quantum states (amplitudes). We are no longer describing objects be they quantum objects; as a matter of fact, this is the trait differentiating the present approach with many others based on a BO scheme. Here, only quantum states are sought. This change goes hand in hand with the view of quantum states sustained by a materiality that is kept fixed while quantum states count in sets of infinite elements. The materiality does not wear a quantum state as a T-shirt, it sustain quantum states without localization [20].

A set of nuclear energy levels tagged with electronic $\{j\}$-labels associated with (electronic) attractors defined by a $\{\xi^{(j)}\}$-geometries complete the model: [1]

$$E_{j,g(j)} = E_j(\boldsymbol{\xi}^{(j)}) + \varepsilon_{g(j)}. \tag{5}$$

The key point concerns these energy levels that *do not* depend upon instantaneous nuclear positions, as it is the case in our semi-classic schemes. These electronuclear quantum numbers contain information needed to analyze the physical-chemical processes of interest.

In spite of the fact that, mathematically, the basis set $\{\Psi_k(\mathbf{q})X_{g(k)}(\boldsymbol{\xi})\}$ is incomplete, the framework can be used to define particular models able to handle most of the experimental situations described in refs. [10–17]. In practice, the separable set should be sufficient whenever the molecular processes can be described with electronic states associated with a *single* I-frame.

However, a simple scattering system such as $H(1s) + H^+$ involves *three* I-frames. Under laboratory conditions several frames can exist, but once chosen, a proper quantum treatment must subsume them into a single one representation (see below).

2.3 Box-basis-states and chemical processes description

A possible avenue to address the above issue is by labeling electronuclear basis functions with quantum numbers formally derived by embedding each I-frame system in the same, auxiliary three-dimensional (3-D) box retaining appropriate quantum numbers for box-states. In a pictorial way, these particle-states are gathered into direct products that preserve the order of elementary constituents (electrons and nuclei).

Consider a sufficiently large box that encloses all relevant laboratory settings one deems necessary to include. If the quantum states (sustained by the material system [20,21]) are embedded into the *same* box, each of them will give rise (separately) to conventional energy-box levels denoted as: $E_{\mathbf{n}(H_2^+)}$, $E_{\mathbf{n}(H)}$, $E_{\mathbf{n}(H^+)}$, where $\mathbf{n}$ is a vector of 3-D box quantum numbers. To ensure commensurability with the electronuclear H_2^+ system base states, combine the latter two into the composite elements required by the laboratory conditions: the associated basis states are direct products of box-states

for the H and H^+ I-frame systems, i.e., $|\mathbf{n}(H)\rangle \otimes |\mathbf{n}(H^+)\rangle$ and $|\mathbf{n}(H^+)\rangle \otimes |\mathbf{n}(H)\rangle$, with energies labeled as $E_{\mathbf{n}(H,H^+)}$ and $E_{\mathbf{n}(H^+,H)}$. Note the symbols H and H^+ do not stand for objects but refer to quantum numbers: any permutations affect quantum numbers and not the order in configuration space. In this context, H^+ is characterized by an implicit "hole" quantum number.

Last but not least, quantized EM fields belonging to the Fock space (photon base states discussed in ref. [22]) that are characteristic of quantum electrodynamics complete the description for laboratory arrangements; its associated basis vectors $|n_\omega\rangle$ are labeled by the number of energy quanta n_ω of frequency ω at disposal in the field [21]. See also Chap. 19 in ref. [22].

2.3.1 Free and entangled radiation/matter states

Select two generic electronic states for H_2^+, $k = 0$ and $k = 1$ and two quantized EM field basis (with angular frequency ω), $\{|n_\omega = 0\rangle \& |n_\omega = 1\rangle\}$) and form two direct product base states:

$$|\mathbf{n}\left(H_2^+\right); k = 0\rangle \otimes |n_\omega = 1\rangle \quad \text{and} \quad |\mathbf{n}\left(H_2^+\right); k = 1\rangle \otimes |n_\omega = 0\rangle, \tag{6a}$$

$E_{\mathbf{n}(H_2^+)}$ is set as the ground-state energy of the box-states. The direct product notation is flexible enough to let us implicitly hint at relative directions, as well as the relative I-frame kinetic energy for the material system; this is good enough for a qualitative analysis. The basis states (6a) are *non-entangled* (free states) and display the same energy. In contrast, *entangled* basis states involving the material system dressed by an EM field would read as follows:

$$|\mathbf{n}\left(H_2^+\right); k = 0; n_\omega = 1\rangle \quad \text{and} \quad |\mathbf{n}\left(H_2^+\right); k = 1; n_\omega = 0\rangle, \tag{6b}$$

The labels embrace all the information. Energy is no longer available to the EM field; the subsystems are non separable. The material base states are then dressed with the EM field constituting a new type of base functions (*at the fence*).

Finally, the entangled quantum states for entire system appear as time-dependent linear superpositions over *all* basis functions; the resulting description involves *one* inertial frame. The presence of entangled states is relevant at the fence space (laboratory) so that care must be exercised in examining time evolution there.

2.3.2 Feshbach quantum states

We have at hand the elements to construct a model basis set. Adjust collision energy for a pair $\left(E_{\mathbf{n}(H)} + E_{\mathbf{n}(H^+)}\right)$ in near-resonance to $E_{\mathbf{n}(H_2^+)}$ states (entangled and non-entangled with the radiation field), the material system sustains linear superposition states of the kind:

$$
\begin{aligned}
|\Psi\rangle &= C_{\mathrm{I}}|\mathbf{n}(H_2^+);k=0\rangle\otimes|n_\omega=1\rangle + C_{\mathrm{II}}|\mathbf{n}(H_2^+);k=1\rangle\otimes|n_\omega=0\rangle \\
&\quad + C_{\mathrm{I}'}|\mathbf{n}(H_2^+);k=0;n_\omega=1\rangle + C_{\mathrm{II}'}|\mathbf{n}(H_2^+);k=1;n_\omega=0\rangle \\
&\quad + C_{\mathrm{III}}|\mathbf{n}(H)\rangle\otimes|\mathbf{n}(H^+)\rangle + C_{\mathrm{IV}}|\mathbf{n}(H^+)\rangle\otimes|\mathbf{n}(H)\rangle + \cdots \\
&\equiv \big(|\mathrm{I}\rangle|\,\mathrm{II}\rangle\,\big|\mathrm{I}'\rangle\big|\,\mathrm{II}'\rangle\,|\mathrm{III}\rangle|\,\mathrm{IV}\rangle\ldots\big)\cdot(C_{\mathrm{I}}\ \ C_{\mathrm{II}}\ \ C_{\mathrm{I}'}\ \ C_{\mathrm{II}'}\ \ C_{\mathrm{III}}\ \ C_{\mathrm{IV}}\ldots)^t
\end{aligned}
\tag{7}
$$

In Eq. (7), the box provides *a single common* I-frame; detectors and/or sources are "located" at boundaries, with their actual positions chosen by the experimenter. Before proceeding with mathematical discussions there is need to introduce a constraint. Namely, the model is reduced to six components and no spontaneous emission takes place. Thus, key information is captured in the amplitudes of the column vector:

$$
(C_{\mathrm{I}}\ \ C_{\mathrm{II}}\ \ C_{\mathrm{I}'}\ \ C_{\mathrm{II}'}\ \ C_{\mathrm{III}}\ \ C_{\mathrm{IV}})^t \tag{8}
$$

The interactions between entangled base states (with amplitudes $C_{\mathrm{I}'}$ and $C_{\mathrm{II}'}$) and asymptotic base states (with amplitudes C_{III} and C_{IV}) sustain generic *Feshbach quantum states*: resonance within discrete and continuum energy levels subset [23].

2.3.3 Quantum states for chemical processes

Consider an initial laboratory condition, e.g., $(0\ \ 0\ \ 0\ \ 0\ \ 1\ \ 0)^t$; this state is sustained by a left-hand-side beam of hydrogen atoms that was setup to colliding with a right-hand-side proton beam. The opposite symmetry state would read: $(0\ \ 0\ \ 0\ \ 0\ \ 0\ \ 1)^t$. These states reflect possible choices in experimental set up. The characteristic of a quantum description is that it enforces the presence (in the base set) of such possibilities.

One of the effects generated by the interaction is a charge (hole) exchange which results in the spatially-entangled quantum state, e.g.: $(0\ \ 0\ \ 0\ \ 0\ \ 2^{-1/2}\exp(i\pi)\ \ 2^{-1/2})^t$. In other words, an detector (observer) located along a direction expecting an H-atom state response can also detect a hole-response (a proton, H^+), and according to the information conveyed by the entangled quantum state it will do it with relative *intensity* 1/2. Thus, even if at the laboratory level the system was prepared in a given possibility after interaction the measured state will show response from the second possibility that is contained in the quantum state.

The event (laboratory level) elicits only one type of response at a time. In simple words, quantum mechanics does not describe particle motions in laboratory (real) space; it describes quantum states sustained by this materiality [20,21].

Consider more carefully the role played by the H_2^+-states in this charge exchange. As done conventionally, one can visualize fragments that propagate in directions that cross at one point at a given time. The relative kinetic energy is selected so that resonance conditions are met with photon field dressed base states. But one can imagine a state where one can distinguish non-zero amplitudes at C_{I} and C_{II} engaging the ground and excited electronic state of H_2^+. Now, either a channel to the entangled state is open so that it may produce the amplitude column vector:

$$(0\ \ 0\ \ C_{\mathrm{I}'}\ \ C_{\mathrm{II}'}\ \ 0\ \ 0\ldots)^t\,; \tag{9}$$

or no interaction takes place, i.e., the initial state of this system remains unchanged in a quantum state with amplitude vector $(C_{\mathrm{I}} \neq 0\ C_{\mathrm{II}} = 0\ \ 0\ \ 0\ \ 0\ \ 0\ldots)^t$.

For the entangled (dressed) case, the system enters time-dependent quantum states sustained by the material system and the EM field in a non-separable manner:

$$|\text{Entangled}, \tau\rangle \Rightarrow (0\ \ 0\ \ C_{\mathrm{I}'}(\tau)\ \ C_{\mathrm{II}'}(\tau)\ \ 0\ \ 0)^t. \tag{10}$$

In Eq. (10), the τ-parameter refers to a sort of proper time (in the sense of special relativity theory) of the entangled quantum state as determined by the laboratory conditions (rather than the familiar laws of time evolution in a single isolated system). It is here that we find the so-called "fence space", i.e., a boundary where Hilbert space and laboratory space must be taken into account [20,21]. From the molecular/atomic point of view we have to handle an open system. There is a constraint we imposed above in order to be able to use Hilbert space time evolution with the rigged base vector $(|\mathrm{I}\rangle\ \ |\mathrm{II}\rangle\ \ |\mathrm{I}'\rangle\ \ |\mathrm{II}'\rangle\ \ |\mathrm{III}\rangle\ \ |\mathrm{IV}\rangle\ldots)$. Namely, no spontaneous emission is allowed in this model and standard time evolution holds. One can now explore the possibilities available.

The advantage we have resides in the nature of the base states that permit discussing also possible events that, of course, suppress time evolution in this rigged Hilbert space.

Thus, the process $(0\ \ 0\ \ 0\ \ 0\ \ 1\ \ 0)^t \ \ \rightarrow (0\ \ 0\ \ C_{\mathrm{I}'}(\tau)\ \ C_{\mathrm{II}'}(\tau)\ \ 0\ \ 0)^t$ corresponds to a possible laboratory event; it is not localizable for a single system, as not every collision results in entanglement. But, once entanglement takes place, the time duration for the opposite process to happen is not predictable in terms of a single-system history either; a number of alternative events can take place. Yet it can be controlled externally (e,g. laser induced emission). However, under the constraint of our model, the time evolution is set up allowing us to examine different possibilities.

For a chemist, a main interest resides in understanding production of ground state H_2^+ response. The system is put in an energy shell above ground state, a mechanism would be a possible (induced) photon-emission process symbolized as:

$$\begin{aligned}(0\ \ 0\ \ C_{\mathrm{I}'}(\tau)\ \ C_{\mathrm{II}'}(\tau)\ \ 0\ \ 0)^t &\rightarrow (0\ \ 0\ \ C_{\mathrm{I}'}(\tau)=1\ \ C_{\mathrm{II}'}(\tau)=0\ \ 0\ \ 0)^t \\ &\rightarrow (1\ \ 0\ \ 0\ \ 0\ \ 0\ \ 0)^t\end{aligned} \tag{11}$$

The final amplitude vector matches the basis state $|\mathbf{n}(H_2^+); k=0\rangle \otimes |n_\omega = 1\rangle$, that we will take now to standing for a photon being emitted from the material system that sustains the quantum state. In other words, the material system is left in the electronic ground state and a photon state "escapes"; this is a form of *decoherence*.

Other possible physicochemical phenomena could also be observed. Viz., while the system shows non-zero amplitude at the entangled state, it can relax to the ground state via vibrational steps (a mechanism that should become more prevalent in complex systems) and this may occur whenever the amplitude $C_{\mathrm{II}'}$ is near unity.

The field-entangled state $(0\ \ 0\ \ C_{\mathrm{I}'}(\tau)\ \ C_{\mathrm{II}'}(\tau)\ \ 0\ \ 0\ \ \ldots)^t$ may also evolve into the spatially-entangled state, e.g. $(0\ \ 0\ \ 0\ \ 0\ \ 2^{-1/2}\ \ 2^{-1/2})^t$, corresponding in chemical

parlance to a charge-hole exchange. The latter quantum state embodies possibilities accessible to the real system. E.g., one could measure a charge along a beam that came initially from the left with to the right will detect zero charge (i.e., a H atom). All this information is read from the wave function by detectors probing the quantum state [20]; of course at the laboratory there is no signal sent between separate detectors in real space.

2.3.4 Quantum reaction mechanisms via Feshbach states

One can now describe the most general reaction processes as follows: Start up from the linear superposition state (entangled state) $(0\ 0\ C_{\mathrm{I}'}\ C_{\mathrm{II}'}\ C_{\mathrm{III}}\ C_{\mathrm{IV}})^t$; This entanglement between a bound molecular state and its asymptotic fragments in the continuum allows us to see the reaction process via a *Feshbach resonance* [23].

The amplitudes entering a general "Feshbach quantum state" $(0\ 0\ C_{\mathrm{I}'}\ C_{\mathrm{II}'}\ C_{\mathrm{III}}\ C_{\mathrm{IV}})^t$ may all be *non-zero* (time evolution is omitted here but is always present unless an event happens). Thus this quantum state results from resonant interaction between a (quasi)-discrete bound level and a number of states in the continuum spectrum. With the notation in Eq. (7) restricted to the first six basis functions, a generic "bond-formation" process that results from two separate beams would be written as:

$$\begin{aligned}(0\ 0\ 0\ 0\ 0\ 1)^t \rightarrow (0\ 0\ C_{\mathrm{I}'}\ C_{\mathrm{II}'}\ C_{\mathrm{III}}\ C_{\mathrm{IV}})^t \rightleftarrows (0\ 0\ C_{\mathrm{I}'}\ C_{\mathrm{II}'}0\ 0)^t \\ \rightleftarrows \left(2^{-1/2}\ 2^{-1/2}\ 0\ 0\ 0\ 0\right)^t . \end{aligned} \tag{12a}$$

Double arrows indicate that the system evolves in time under quantum mechanical law. End result being a linear superposition of dressed ground and first-excited states sustained by the materiality of H_2^+. Decoherence yielding $(1\,0\,0\,0\,0\,0)^t$ viz. a photon possibly emitted in a random direction.

Similarly, a generic "bond-breaking" process starting from a dressed ground state would appear as:

$$\begin{aligned}(1\ 0\ 0\ 0\ 0\ 0)^t \rightarrow (0\ 0\ C_{\mathrm{I}'}\ C_{\mathrm{II}'}\ 0\ 0)^t \rightleftarrows (0\ 0\ C_{\mathrm{I}'}\ C_{\mathrm{II}'}\ C_{\mathrm{III}}\ C_{\mathrm{IV}})^t \\ \rightleftarrows \left(0\ 0\ 0\ 0\ 2^{-1/2}2^{-1/2}\right)^t . \end{aligned} \tag{12b}$$

A laboratory output is the entangled state involving at laboratory space two spatially separated beams.

For these cases (Eq. 12a, b), a Feshbach quantum state plays the pivotal role for directing chemical change and entanglement. In a semiclassic picture, the photon energy required to "activating" H_2^+ by dressing its ground electronic state at the end would appear as part of the relative kinetic energy.

The preceding discussions illustrate typical quantum situations associated to the present model. Now we move on from abstract quantum analyses to contact with more traditional manners to describe chemical processes yet keeping the quantum flavor. So far we have done this with analytical semi-classic situations [4–9].

3 Bridging attractors and asymptotic states

For chemical processes as those for instance discussed by Butler [25] we have to link bound states to a variety of asymptotic states representing possible reactants (products). The standard manner used with adiabatic procedures is no longer an option. We proceed as follows.

The electronic energy given in Eq. (5) comes out as variational solution leading to the equation [7–9]:

$$\hat{H}_e\left(\hat{\mathbf{q}};\boldsymbol{\xi}^{(j)}\right)\psi_k^{(j)}(\mathbf{q}) = E_k(\boldsymbol{\xi}^{(j)})\psi_k^{(j)} = E_k^{(j)}\psi_k^{(j)}, \tag{13}$$

The electronic base function $\psi_{k=0}{}^{(j)}(\mathbf{q})$ determines the stationary geometry $\boldsymbol{\xi}^{(j)}$ (cf. [1–9] for details). More interesting, the sets $\{E_k^{(j)}\}$ and $\{E_k^{(n)}\}j \neq n$ in principle includes the same diabatic eigen functions ordered in a different manner [7–9]. These electronic functions are characterized by their nodal distributions. Using an appropriate ordering procedure organize the information with sets of $E_{j,g(j)}$ that counts all meaningful states.

Thus the set $\{E_{j,g(j)}\}$ and $\left\{\phi_{j,g(j)}\right\}$ provides labels attached to chemical species via the auxiliary diabatic determination. They form a subset of a complete set of bound eigen states for the total Hamiltonian: $\hat{H} = \hat{K}(\boldsymbol{\xi}) + \hat{H}_e\left(\hat{q},\boldsymbol{\xi}\right)$ Hamiltonian $\hat{H}$ is diagonal in the $\left\{\phi_{j,g(j)}\right\}$-basis set. This is one of the key feature this model has [1–9].

Thus, the energy eigenvalues are independent from the instantaneous nuclear positions. This fact will be used to construct more advanced models in Sect. 5.

3.1 Electronic states model prompted by external fields

With the diabatic-basis model compute the quantum superposition states denoted as $|\Phi\rangle$ in presence of external fields; Φ are eigen functions of the electronic Hamiltonian in the field $\hat{H}_{\text{full}}$:

$$\hat{H}_{\text{full}} = \hat{H}_e\left(\hat{q},\boldsymbol{\xi}\right) + \hat{V}_{\text{e-field}} \tag{14}$$

Symbol $\hat{\mathbf{p}}$ is the electronic momentum operator; $\mathbf{A}$ is the electromagnetic vector potential. The electronuclear functions $\{\Phi(\mathbf{q};\boldsymbol{\xi})\}$-functions depend of the applied external electric field through $\mathbf{A}$:

$$\Phi(\mathbf{q};\boldsymbol{\xi}) = \sum_k C_k(\mathbf{A},\boldsymbol{\xi})\psi_k(\mathbf{q}). \tag{15a}$$

The two open-shell bases $\{\psi_i\}$-functions differ in parity; ψ_1 resembles a σ_g molecular orbital and ψ_2 correlates with a σ_u orbital at $x \to \infty$. The different symmetry makes it possible to couple these functions with an external electric field [1,2].

3.2 Floating Gaussian orbitals grid method

Mapping quantum and semiclassic schemes requires strict conservation of the electronic quantum number in order to interpret the $|\Psi\rangle$-states in external fields; this ensures that the nuclear configurations affect *only* the $\{C_j\}$-amplitudes (cf. Eqs. (1) and (4)). To this end, use a set of grid-fixed floating orbitals to build $abinitio\{\psi_j(\mathbf{q})\}$-functions; this procedure ensures that the pattern of nodal planes in each ψ_j $(\mathbf{q})$-function is maintained over $\boldsymbol{\xi}$-space (i.e., they become "diabatic" functions [26]).

3.2.1 Optimized grid for the two-state description of the $H_2^+ \rightarrow H(1s) + H^+$ process

In the case of bond breaking, the "product-state" attractor is asymptotic; its calculation requires a grid with a different symmetry from that used for the "reactants" (here, H_2^+). Otherwise, the *same type and number of orbitals* are used for *all* reactants and products.

Consider a three-point grid to study the $H_2^+ \rightarrow H(1s) + H^+$ process. Calculations are performed with Gaussian 98 (G98) program [27] adapted to the present protocol. Grid points are "ghost atoms" (denoted as *Bq*, for "Banquo atoms"). Each "*Bq*-atom" is assigned an explicitly defined cc-pV-5Z [*5s4p3d2f1g*] basis set. A nonstandard option in G98 allows us to include the H^+ nuclei as a background of two positive charges acting on three *Bq*-atoms.

The j-invariant U_1-potential for the "reactant" $|H_2^+\rangle$-species is computed as follows:

(a) First, set the three FGOs collinearly along the x-axis. One of the *Bq*-atoms becomes the origin; the other two are placed at $(\pm x_o,0,0)$. Initially, two positive (H^+) charges are set over these *Bq*-atoms; floating orbitals and charges are then moved jointly so as to minimize the energy with respect to x_o. The cc-pV5Z basis set gives $x_o^* = 0.52847$ Å as optimal separation. This value defines $U_1(\boldsymbol{\xi}^{(1)})$, the minimum for the $|H_2^+\rangle$-attractor. The resulting density matrix gives the ψ_1-function for all $\boldsymbol{\xi}$-geometries. The equilibrium bond length $r_{BB}^* = 2x_o^* = 1.05694$ Å and minimum energy $minU_1(\boldsymbol{\xi}) = -0.602626$ a.u. match the "exact" results (1.05677 Å and −0.602634 a.u., respectively [28]).

(b) Next, the FGOs are frozen at their optimized positions. Table 1 gives the corresponding spin density matrix for the three "ghost-atoms." With this information, the potential energy function U_1 is built by moving the two H^+ charges, while keeping the three-point *Bq*-grid fixed. For simplicity, we study $U_1(x)$, where x is the distance between two H^+ charges symmetrically placed with respect to the *Bq*-atom at the origin. Figure 1 (diagram 1*a*) shows the arrangement for $U_1(x = 2)$: the *Bq*-orbitals are denoted by open circles (at a fixed distance $r_{BB}* \approx 1.057$ Å); the H^+ charges appear as shaded circles. Figure 2 shows the resulting potential energy function $U_1(x)$ for the $|H_2^+\rangle$-species; the square "1*a*" corresponds to the U_1 value for the arrangement displayed in Fig. 1.

(c) The "product-state" involves an asymptotic fragment with no electrons, i.e., an infinitely separated H^+ charge. The corresponding attractor is built with a *distinct*

Table 1 Spin-density matrix associated with the electronic molecular $|H_2^+\rangle$-state (i.e., the "diabatic reactant") as represented with a three-point grid of floating orbitals in the cc-pV5Z basis set, comprising 165 basis functions

	Bq_1 (left)	Bq_2 (centre)	Bq_3 (right)
Bq_1 (left)	0.218042	0.081472	0.094502
Bq_2 (centre)	0.081472	0.049025	0.081472
Bq_3 (right)	0.094502	0.081472	0.218042

The symbols Bq_i represent the orbitals (i.e., "ghost atoms") at the positions depicted in Fig. 1. These locations are optimized to produce the lowest-energy minimum for the H_2^+ ground-state potential energy attractor (see text for the geometry). These locations are never modified during the computation of the "reactant" effective potential energy function $U_1(x)$ (i.e., the spin densities are constant for all x values)

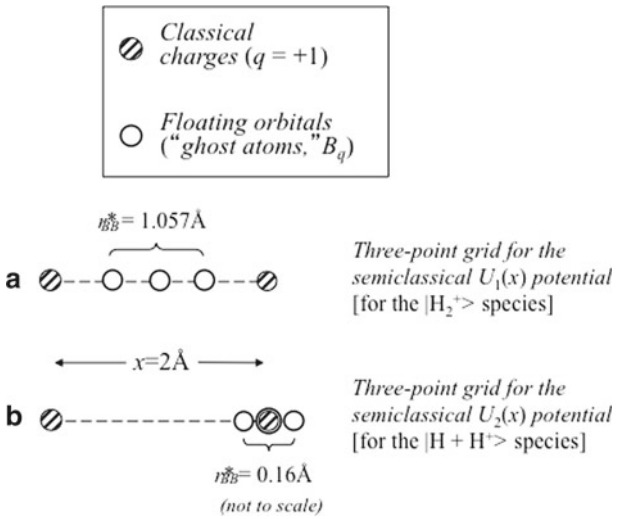

Fig. 1 Construction of electronic basis functions using a three-point grid of floating orbitals. This description comprises two charges (the H^+ nuclei, denoted by shaded circles) and three floating Gaussian functions (denoted by open circles). The location of these orbitals (or "ghost atoms") is optimized so as to produce a minimum potential energy for the molecular $|H_2^+\rangle$-attractor (case 1a) and the asymptotic $|H + H^+\rangle$-attractor (case 1b). We derive the semiclassical potential energy $\{U_i(x)\}$-functions by keeping the orbital grid fixed and placing the nuclear charges at various x-separations

three-point grid, depicted in Fig. 1 (diagram 1b). Here, one of the H^+ charges is placed at the central Bq-atom, and the other two floating orbitals to its left and right (cf. Fig. 1a). Next, we optimize their separation so as to provide the lowest energy for a single $H(1s)$ atom. The optimal separation is 0.16 ± 0.01 Å (cf. Fig. 1b), which produces an energy $minU_2 = -0.499995$ a.u. with the cc-pV5Z basis set, thereby matching (a) in accuracy.

(d) The k-invariant $U_2(x)$ potential energy function for the "products" is computed as in (b), i.e., from a ψ_2-function built with the fixed grid optimized in (c). The resulting $U_2(x)$ potential appears in Fig. 2, where the right-hand side charge is placed atop the central Bq-atom. The asymptotic dissociation channel has a minimum only in the limit $x \to \infty$ [8].

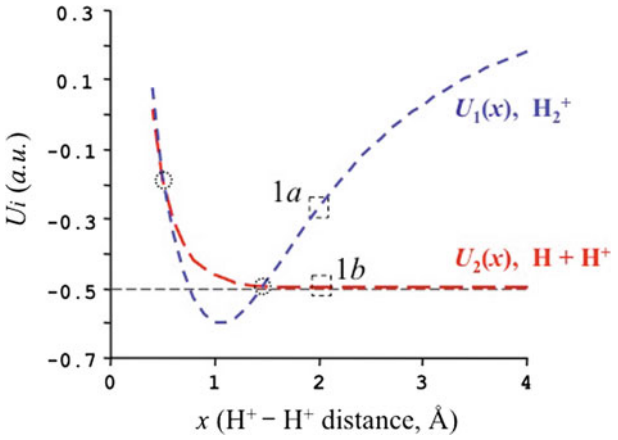

Fig. 2 Semiclassical potential energy functions built with fixed orbital grids. The configurations "1a" and "1b" correspond to those in Fig. 1 for the reactant and product states, respectively. The dashed circles stand for the "diabatic crossings" between the curves $U_1(x)$ and $U_2(x)$. The crossing at $x_{DC} \approx 1.4$ Å represents the region with rapid change in quantum-state amplitudes; it is associated with the occurrence of a barrier for bond breaking. The total energy is given by $\hat{H}_{\text{full}}\Phi(\mathbf{q};\boldsymbol{\xi}) = E_{\text{full}}(\boldsymbol{\xi})\,\Phi(\mathbf{q};\boldsymbol{\xi})$

In Sect. 4, we use these $\{U_i(x)\}$-potentials to build the superposition quantum states in an external electric field.

3.2.2 Semi-classic quantum states

The diabatic electronic basis permits construction of linear superpositions. The total energy for this model is given by

$$\hat{H}_{\text{full}}\Phi(\mathbf{q};\boldsymbol{\xi}) = E_{\text{full}}(\boldsymbol{\xi})\,\Phi(\mathbf{q};\boldsymbol{\xi}).$$

Employ the matrix element $V_{12} = \langle\psi_1(\mathbf{q})|\hat{V}_{\text{e-field}}\psi_2(\mathbf{q})\rangle_q$ as a parameter proportional to the applied field [28]. This implicitly plays the role of the quantized EM field coupling. The Eq. (15a) becomes:

$$\Phi(\mathbf{q};x) = C_1(x)\,\psi_1(\mathbf{q}) + C_2(x)\,\psi_2(\mathbf{q}). \tag{15b}$$

The different parity implies $\langle\psi_1|\hat{H}_e(\hat{\mathbf{q}},\boldsymbol{\xi})\psi_2\rangle_q = 0$ and $\langle\psi_i|\hat{V}_{\text{e-field}}\psi_i\rangle_q = 0$, with $i = 1, 2$. Therefore, the only nonzero Hamiltonian matrix elements are [cf. Eqs. (6,7)]:

$$\langle\psi_1|\hat{H}_{\text{full}}\psi_2\rangle_q = V_{12}; \quad \langle\psi_i|\hat{H}_{\text{full}}\psi_i\rangle_q = U_i(x). \tag{16}$$

The lowest eigenvalue of the $\hat{H}_{\text{full}}$-matrix gives the effective potential energy function [7]:

$$E_{\text{full}}(x) = \langle \Phi(\mathbf{q}; x)|\hat{H}_{\text{full}}\Phi(\mathbf{q}; x)\rangle_q$$
$$= U_1(x) + 1/2\{\Delta U_{12}(x) - |\Delta U_{12}(x)|\sqrt{[1 + 4(V_{12}/\Delta U_{12}(x))^2]}\} \quad (17)$$

The energy gap: $\Delta U_{12}(x) = U_2(x) - U_1(x)$. Finally, the amplitudes in the superposition states are [7–9]:

$$|C_2(x)| = 1/\sqrt{\{1 + (V_{12}/[E_{\text{full}}(x) - U_1(x)])^2\}}, \quad |C_1|^2 + |C_2|^2 = 1. \quad (18)$$

By varying the charge separation x introduced within state-fixed floating Gaussian model, we can study how the external coupling V_{12} affects the function in Eq. (15b).

In Fig. 2, the dashed circles stand for the "diabatic crossings" between the curves $U_1(x)$ and $U_2(x)$. The crossing at $x_{DC} \approx 1.4$ Å represents a region with rapid change in quantum-state amplitudes as elicited in Fig. 3. This crossing is associated with the occurrence of a barrier for bond breaking; Fig. 4 show this in more detail.

A $V_{12} \neq 0-$ value produces a $E_{\text{full}}(x)$-curve that interpolates between the two attractors and produces a rapid switch in $|C_i|^2$-intensities near the $x_{DC} \approx 1.4$ Å "diabatic crossing" in Fig. 2.

A nonzero amplitude in the product $|H(1s)H^+\rangle$-state appears thus even in the neighborhood of reactant-like geometries; this would correspond to a projected Feshbach state as it was introduced in Sect. 2.3.3 once the model is extended, for example see Sect. 5.

Figure 3 illustrates the typical behavior predicted by our two-state model at *high-field* intensities. The results correspond to $V_{12} = 0.05$ a.u., and they depict the $E_{\text{full}}(x)$-curve (top) and the superposition amplitudes $|C_i|$ (bottom) as functions of the charge separation x. For clarity, we show also the model $U_i(x)$ potentials. Two important observations can be made:

i At high fields, the effective energy increases monotonically from a reactant-like quantum state at $x \approx 1.1$ Å to the asymptotically separated fragments.
ii The electronic basis ψ_1-function dominates the superposition quantum state in the vicinity of the U_1 minimum, yet the ψ_2-contribution is still substantial. Note also that the actual location of the global minimum for $E_{\text{full}}(x)$ is shifted to larger values (i.e., *the bond lengthens as a result of the applied field*). A similar bond stretching by laser fields has been reported in simple molecules [29]. For $x \rangle x_{DC} \approx 1.4$, we observe a marked switch in amplitudes. Note, ψ_1-function contributes much less to the asymptotic "product" quantum state than the ψ_2-function contributes to the "reactant" quantum state.

A quantum physical description as given in Eq. (12a) can be "visualized" with this figure. The extension covered by the asymptotic component (shaded region) will make increase the "bond length" beyond the one yielded by a semiclassic picture.

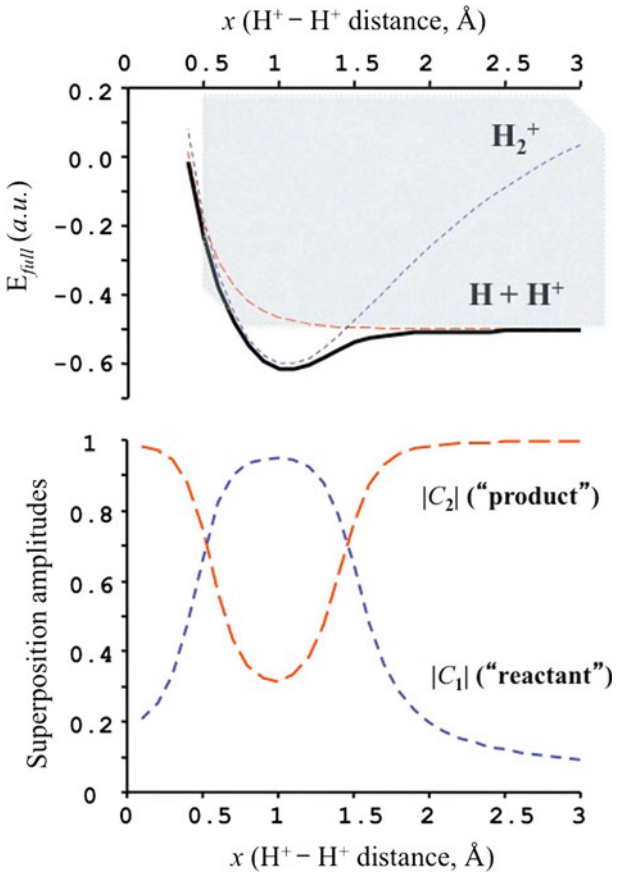

Fig. 3 This figure contains two levels of information. First, effective potential energy in the field, $E_{\text{full}}(x)$, and superposition amplitudes $\{|C_i|\}$, obtained when using an external coupling with a matrix element $V_{12} = 0.05$ a.u. This is a typical "high-field" behaviour with no barrier. It presents a strong contribution of the product $|H + H^+\rangle$-state amplitude in the region of the molecular $|H_2^+\rangle$-reactant state. Note also the effective "softening" of the H_2^+-bond in the field, as represented by a shift in the bond length around the global minimum for the non-isolated electronic system. Second, the quantum scheme does not require of potential energy functions. Instead, a set of discrete levels, e.g. $E_{j=0,g(0)} = E_{j=0}(\boldsymbol{\xi}^{(0)}) + \varepsilon_{g(0)}$ (ro-vibration model) not explicitly shown. A rectangular domain where the discrete states are immersed suggests a continuum for the dissociated state. For the excited electronic level, just above dissociation energy limit, i.e. $E_{j=1,g(1)}$, the coupling with this continuum contributes to the Feshbach quantum states discussed in the text

While the above pattern characterizes a nonzero V_{12}-coupling, the qualitative behavior varies with the field intensity. Figure 4 highlights the results for $E_{\text{full}}(x)$ in the region near the x_{DC} crossing.

After the barrier there is a shallow minimum at large H^+-charge separations. Its location varies from $x_{min} \approx 2.9$ Å for $V_{12} = 0.010$ a.u. to $x_{min} \approx 2.1$ Å for $V_{12} = 0.019$ a.u., before it disappears at the critical ${V_{12}}^{(c)}$-value. This minimum resembles the trapping of $H(1s) + H^+$ fragments believed to take place during the dynamics of H_2^+ in intense laser fields [30]. Indeed, simulations of H_2^+ dynamics dressed in a

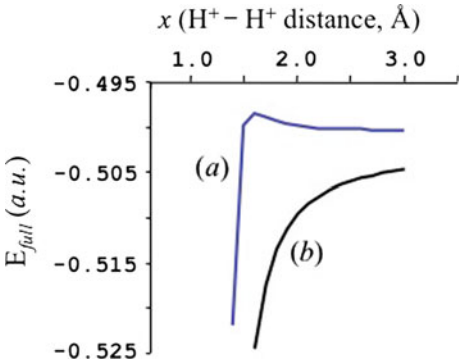

Fig. 4 The curve (*a*) corresponds to $V_{12} = 0.01$ a.u., while the curve (*b*) corresponds to the case $V_{12} = 0.05$ a.u. The results show that there is an *effective barrier* for the process at sufficiently low external fields. In the case of curve (*a*), the barrier for bond *formation* (i.e., $H(1s) + H^+ \rightarrow H_2^+$) is ca. 1.3 kcal/mol. The barrier decreases with the field intensity; our model predicts a critical coupling for a barrierless process $V_{12}^{(c)} \approx 0.02$ a.u. At $V_{12} = 0.019$ a.u., the last detectable barrier is located at $x = 1.95$ Å and it is vanishingly small for the $H(1s) + H^+ \rightarrow H_2^+$ reaction (ca. 10^{-6} a.u.). Change in the geometry of the effective $E_{\text{full}}(x)$-energy as a function of the external coupling. (Only the region around the $U_1 = U_2$ crossing $x_{DC} \approx 1.4$ Å is highlighted). A barrier appears at low fields ($V_{12} = 0.01$ a.u., case (1*a*)), but it is absent at higher external couplings ($V_{12} = 0.05$ a.u., case (1*a*)). We estimate the critical coupling for a barrierless bond breaking in H_2^+ as $V_{12}^{(c)} = 0.02$ a.u.

laser field suggest that the ground state can be trapped in a region satisfying $x \geq 3$ Å at laser intensities ca. 4×10^{13}W/cm^2 [31].

3.3 Quantum chemical mechanistic aspect

The semi-classic computations reported above basically illustrate diabatic behavior. And now we can qualitatively examine some aspects of the quantum mechanistic elements from preceding sections.

There is a ladder if vibration mode centered at the attractor structure characteristic of the quantum states associated to H_2^+. In view of the apparent anharmonicity the domain where the vibration function is well defined becomes larger and larger. Besides these states one should count rotational levels associated to the vibronic levels. These levels are immersed in the dissociation continuum as suggested in the picture.

About and above the dissociation limit the vibronic levels start sensing the continuum related to the asymptotic states. Figure 3 can be seen as pointing to the region where Feshbach quantum states become accessible. In so far time evolution keep the system wandering in that amplitude space there is a delocalization of the nuclear states well beyond classical limits; at $x \approx 1.4$ there are non-zero amplitudes in both channels. As laser energy increases the energy shell locates well above dissociation limit; things appear as if the bonding of $H^+ - H^+$ becomes floppy. Observe that, provided no spontaneous emission takes place the quantum state keeps a "bonding" pattern. We cannot say where the protons are located except that they appear to be trapped by quantum effects.

4 Abstract quantum models: closing a loop

The semi-classic diabatic scheme discussed above provides a subset of basis functions and energy levels where the key information resides in the set of quantum numbers. Formally, a nuclear kinetic energy operator $\hat{K}(\boldsymbol{\xi})$ is added to Eq. (14). The key step is to go back and retain the abstract view for the nuclear configuration space. The total Hamiltonian reads as:

$$\hat{H} = \hat{K}(\boldsymbol{\xi}) + \hat{H}_e(\hat{\mathbf{q}}, \boldsymbol{\xi}) \cdot \tag{19a}$$

The spectra within this extended model is given by Eq. (5): $E_{j,g(j)} = E_j(\xi^{(j)}) + \varepsilon_{g(j)}$. Introduce now the quantum numbers to construct a molecular (abstract) basis set: $\{|E_{j,g(j)}\rangle\}$. In so doing, the semiclassic picture is replaced by a quantum scheme. Consequently the Hamiltonian may be represented as:

$$\hat{H} \rightarrow \Sigma_{j,g(j)} E_{j,g(j)} |E_{j,g(j)}\rangle\langle E_{j,g}(j)| \tag{19b}$$

In a way, one gets rid of classical mechanical variables yet chemical structural information is gleaned with the diabatic scheme as developed in the works from our group. The electronic quantum number is the carrier of structural information for the present approach.

For chemical systems susceptible to dissociate/associate there are base states belonging to the continuum of a particular dissociation limit, E_d. The model Hamiltonian containing this novel information can be written as:

$$\hat{H} \rightarrow \Sigma_{j,g(j)} E_{j,g(j)} |E_{j,g(j)}\rangle\langle E_{j,g(j)}| + \int_{Ec}^{E} dE' |E'\rangle\langle E'| \tag{20}$$

The upper limit is controlled by the requirements of the experimental situation. Figure 3 should be seen as a stack of energy levels below and above dissociation limit for H_2^+ ground state. The levels immersed in the continuum (shaded region) via interaction acquire an energy width that corresponds to a quantum state extending beyond the semiclassic bounds. The quantum Feshbach state belongs to this manifold.

These are the elements required to constructing a computation scheme relating laboratory issues to the abstract quantum mechanical models (see below).

5 Quantum dynamical simulations at laboratory level

5.1 Quantum states sustained by a material system

For the hydrogen atom total spin $K = J + I = 0, 1$ while the proton states $\mathrm{I} = 1/2$. Bound states are identified by $K = 1/2, 3/2$ corresponding to spin doublet and quadruplet states.

Asymptotic base states show a generic form: a plane waves multiplied by an internal quantum base state, say, $\exp(i\mathbf{k}.\mathbf{x})|K\,M_K\rangle$. Generic proton states $\exp(i\mathbf{k}'.\mathbf{x}')|I\,M_\mathrm{I}\rangle$. Implied here is the origin for the respective I-frames that identify the source locations. The system is reduced to one-I-frame situation by selecting common boxes and a procedure similar to the one presented in Sect. 2.3 is assumed.

The electronic internal state is signaled by a corresponding quantum number: e.g. $\exp(i\mathbf{k}.\mathbf{x})|K\,M_K, E'\rangle$ for beam states and $|K\,M_K, E_{j(k),g(j)}\rangle$ for bound states. The information is transported by the base states. For the proton, the base states are signaled by the intrinsic angular momentum quantum number (internal state) and the box quantum numbers in a manner similar to that presented in Sect. 2.3.

The direct product base states $|I, M_\mathrm{I}, \mathbf{n}(H^+)\rangle\otimes|K\,M_K, \mathbf{n}(H)\rangle$ include information via the symbols identifying box quantum numbers. The bound state base functions include data on the internal quantum state: $|K\,M_K, \mathbf{n}(H_2^+); E_{j,g(j)}\rangle$. Thus $\mathbf{n}(H_2^+)$ refers to the kinetic energy one can put on the I-frame; for $\mathbf{n}(H_2^+) = \mathbf{0}$ the energy involved is indicated by the internal eigenvalue.

Going back to Fig. 3 it is apparent that the diabatic H_2^+ state sustains a vibration-rotation set of energy levels that now are embedded in the continuum of asymptotic states; also suggested is the dissociation continuum. Those discrete levels found about and above the crossing level will couple to the continuum takes to form linear superpositions; from our structural chemical view point the probing will show a very large zone occupied by the heavy elements (protons). This quantum physical effect is one that is missing in standard semi-classic pictures.

This concludes the preparation of a chemical base set for an open system. To each attractor there is an energy ladder of levels related to nuclear degrees of freedom.

It is worth to insist that a second quantization like formalism can be done in the present context because only quantum numbers matter. The material elements must be present in order to sustain quantum states changes yet they are not localized in a quantum chemical sense.

A subtle element concerns the nature of the abstract quantum numbers. Although we know of their parenthood due to the construction method these numbers are not "vibronic" quantum numbers. The reason is simple: quantum mechanics does not describe the motions of particle in real space; yet in a full-fledged semi-classic scheme [32] the name appears logic.

5.2 Quantum simulation framework

At the laboratory the total Hamiltonian includes external fields. For the model calculations reported above this operator was named as $\hat{H}_\mathrm{full}$, now it is renamed as:

$$\hat{H}_\mathrm{laboratory} = \hat{H} + \hat{V}_\mathrm{e-field} + \cdots \tag{21}$$

The reason is simple, because $\hat{H}$ is introduced via Eq. (19b) or more properly, Eq. (20) that is able to purport spectral laboratory information as well.

The operators $\hat{V}_{\mathrm{e-field}} + \cdots$ stand for all possible types of experimental situations one might be analyzing. This operator must be cast in terms of creation/annihilation operators when the quantized EM is included.

In practical computations we first construct a secular equation with operators (20) and (21). The dimension of the matrix is, in principle, infinite by infinite. External conditions are used to select "slices" of finite dimensions and the scheme becomes adaptable to simulations.

Note that it is operator (21) with Hamiltonian (20) that relates to the representation given in Eq. (7) Sect. 2.3.2 Following this procedure, the explicit particle representation is hidden so that it serves the computational purpose basically.

At this point it is natural to let in non-classical degrees of freedom such as half-integer spin angular momenta in the basis set as it was done in the preceding section.

Now, *the transition matrix elements parametrically depend upon experimental conditions*. This is one of the key features introduced with the help of this abstract formalism. The quantum states obtained stands for the response towards further probes. This is one of the characteristics of quantum systems under modulations with external probing devices.

Thus, the scheme proposed here appears to be apt to implement simulation procedures to be discussed elsewhere.

6 Final comments and conclusions

The present quantum methodology views chemical processes as akin to electronic "transitions," i.e., they involve changes in coherent quantum states modulated by applied fields, in particular electromagnetic ones. Reaction channels are opened by the system's ability, under external steering, to develop large amplitude at a particular electronic base state designated as "product." The present approach seeks to be consistent with modern quantum technologies to control molecular systems [10–17] with all their promise to manipulate structure and reaction mechanisms [15,33] via spatial confinement and electromagnetic fields.

The emerging physical picture discussed in this paper is centered on the role of Feshbach quantum states for material systems entangled with the radiation field. These resonance states act as gates to change amplitudes at entangled bound base states, as well as exit towards entangled asymptotically separated molecular states, thereby emphasizing the quantum physical nature of chemical bond reshuffling processes. The semiclassic (diabatic) model reinforces the qualitative views. Feshbach quantum state may appear to be a quantum path to describe bond reshuffling in general bond alteration processes. This hypothesis is to be tested in further studies.

The model attains a quantum mechanical structure that make it adaptable to the study of quantum impurity models as described in ref. [34]. Thus, we might be able to wed information coming from advanced quantum chemical sources to, for example, continuous-time Monte Carlo methods to study quantum impurity models.

Note that among the steps required to re-construct a quantum picture starting from the semi-classic model quantization of translational energy plays a key role. This issue

is entering again as shown by Toutounji's work [35] in the realms of quantum as well as mathematical chemistry.

Summing up, theoretical developments and non-routine computations results can hence relate directly to experiment, which gives an encouraging perspective. However, the quantum nature of matter defies the classical intuition; and one of the reasons for this state of affair originate by interactions with external probing expresses via matter-sustained quantum states and not as a material object. Quantum physics by addressing, in principle, all possible quantum states resulting from interactions brings novelties that are difficult to digest and assimilate within current forms of interpreting quantum mechanics. Thus, mathematical chemistry becomes an essential framework to mediate different levels of presence for material systems [20,21].

Acknowledgments G.A.A. acknowledges support by NSERC (Canada) and the continued hospitality of the Department of Physical and Analytical Chemistry (Uppsala).

References

1. G.A. Arteca, O. Tapia, Phys. Rev. A **83**, 032311 (2011)
2. O. Tapia, Adv. Quantum Chem. **56**, 31 (2009)
3. O. Tapia, P. Braña, J. Mol. Struct. (Theochem) **580**, 9 (2002)
4. G.A. Arteca, O. Tapia, Int. J. Quantum Chem. **107**, 382 (2007)
5. G.A. Arteca, J.P. Rank, O. Tapia, J. Theor. Comput. Chem. **6**, 869 (2007)
6. G.A. Arteca, J.P. Rank, O. Tapia, Int. J. Quantum Chem. **108**, 651 (2008)
7. G.A. Arteca, O. Tapia, J. Math. Chem. **37**, 389 (2005)
8. G.A. Arteca, O. Tapia, J. Math. Chem. **35**, 1 (2004)
9. G.A. Arteca, O. Tapia, J. Math. Chem. **35**, 159 (2004)
10. J.I. Cirac, P. Zoller, Phys. Today **57**, 38 (2003)
11. R. Côté, Nat. Phys. **2**, 583 (2006)
12. D. DeMille, Phys. Rev. Lett. **88**, 067901 (2002)
13. A. André, D DeMille, J.M. Doyle, M.D. Lukin, S.E. Maxwell, P. Rabl, R.J. Schoelkopf, P. Zoller, Nat. Phys. **22**, 636 (2006)
14. Y. Xia, L. Deng, J. Yin, Appl. Phys. B **81**, 459 (2005)
15. R.V. Krems, Int. Rev. Phys. Chem. **24**, 99 (2005)
16. R.V. Krems, A. Dalgarno, Phys. Rev. A **68**, 013406 (2003)
17. S. Cornish, Physics **1**, 24 (2008)
18. O. Tapia, in *Beyond Standard Quantum Chemical Semi-classic Approaches: Towards a Quantum Theory of Enzyme Catalysis*, ed. by P. Paneth, A. Dybala-Defratyka. Kinetics and Dynamics, Challenges and Advances in Computational Chemistry and Physics, vol. 12, pp. 267–298 (2010)
19. R. Crespo, M.-C. Piqueras, J.M. Aulló, O. Tapia, Int. J. Quantum Chem. **111**, 263 (2011)
20. O. Tapia, Adv. Quantum Chem. **61**, 49 (2011)
21. O. Tapia, *Quantum Physical Chemistry: Basic Quantum Mechanics for Process Description.* http://www.pac.uu.se/Fysikalisk_kemi/Personal/Emeritus/Orlando_Tapia-Olivares/
22. L.E. Ballentine, *Quantum Mechanics: A Modern Development* (World Scientific, Singapore, 1998)
23. M. Born, K. Huang, *Dynamical Theory of Crystal Lattices* (Oxford, 1956).
24. H. Feshbach, Ann. Phys. **5**, 357 (1958)
25. L.J. Butler, Annu. Rev. Phys. Chem. **49**, 125 (1998)
26. T. Helgaker, J. Almlöf, J. Chem. Phys. **89**, 4889 (1988)
27. M.J. Frisch et al., *Gaussian 98 [Revision A.7]* (Gaussian Inc., Pittsburgh (USA), 1998)
28. D.R. Bates, R.H.G. Reid, At. Mol. Phys. **4**, 13 (1968)
29. A. Hishikawa, A. Iwamae, K. Yamanouchi, Phys. Rev. Lett. **83**, 1127 (1999)
30. H. Posthumus, J. Rep. Prog. Phys. **67**, 623 (2004)
31. A. Giusti-Suzor, F.H. Mies, L.F. Di Mauro, E. Charron, B. Yang, J. Phys. B **28**, 309 (1995)
32. M. Stroe, M. Fifiring, Mol. Phys. **109**, 1617 (2011)

33. J.R. Levis, G.M. Menkir, H. Rabitz, Science **292**, 709 (2001)
34. E. Gull, A.J. Millis, A.I. Lichtenstein, A.N. Rubtsov, M. Troyer, Ph. Werner, Rev. Mod. Phys. **83**, 349 (2011)
35. M. Toutouni, Int. J. Quantum Chem. **111**, 3475 (2011)